Supporting Information for:

# Surprisingly Long-Lived Ascorbyl Radicals in Acetonitrile: Concerted Proton-Electron Transfer Reactions and Thermochemistry

Jeffrey J. Warren and James M. Mayer*

*University of Washington, Department of Chemistry, Campus Box 351700, Seattle, Washington 98195*

mayer@chem.washington.edu

**General Experimental.** All solutions were prepared in a nitrogen filled glovebox unless otherwise noted. Reagents were purchased from Aldrich, with the exception of (1,8-diazabicyclo[5.4.0]undec-7-ene) (DBU, Strem). 1,5,7-Triazabicyclo[4.4.0]dec-5-ene (TBD) was purified by sublimation under reduced pressure and stored in an $N_2$ filled glovebox. TEMPOH was synthesized from TEMPO$^{\bullet}$ following the literature procedure.[1] 2,4,6-Tri-*t*-butylphenoxyl ($^{t}Bu_3PhO^{\bullet}$) and 2,6-di-*t*-butyl-4-methoxy phenol were synthesized as previously described.[2] 2,6-Di-*t*-butyl-4-methoxy phenol was isolated as an oil and stored/used as a 0.2 M stock solution in benzene. Tetrabutylammonium hexafluorophosphate ($^{n}Bu_4NPF_6$) was recrystallized 3 times from absolute ethanol, and dried in vacuo for 10 hours at 100 °C. Alumina was activated by drying at 120 °C under vacuum for one day. Unless otherwise noted, acetonitrile solutions of 5,6-isopropylidene ascorbate (***i*AscH$^-$**) were prepared under an inert atmosphere by addition of one equivalent of DBU to solutions of 5,6-isopropylidene ascorbic acid (***i*AscH$_2$**). No significant differences were observed between the reactions of ***i*AscH$^-$** prepared in this fashion versus isolated $^{n}Bu_4NAscH$. $^{n}Bu_4N^+$(*L*-Ascorbate) (***L*-AscH$^-$**) was prepared by addition of 1 equivalent of $^{n}Bu_4NOH$ (1M in $CH_3OH$) to a methanol solution of *L*-ascorbic acid (***L*-AscH$_2$**), following the previously described procedure.[3]

Acetonitrile was used as received from Burdick and Jackson (low water) and was stored in an argon pressurized stainless steel drum, plumbed directly into a glovebox. Other solvents were purchased from Fischer; deuterated solvents were purchased from Cambridge Isotope Labs. $CH_2Cl_2$ and DMSO were dried using a "Grubbs type" Seca Solvent System installed by GlassContour.[4] DMSO was further purified by distillation from activated alumina. Methanol was dried by addition of $Na^0$ followed by fractional distillation. Trifluoroacetic acid was dried by distillation from trifluoroacetic anhydride.

**Instrumentation.** $^1$H NMR spectra were obtained on Bruker AV300, AV301, DRX499 or AV500 spectrometers at 298 K, unless otherwise noted. Chemical shifts are reported in ppm relative to TMS by referencing to residual solvent. EPR spectra were collected at ambient

(1) Mader, E. A.; Davidson, E. R.; Mayer, J. M. *J. Am. Chem . Soc.* **2007**, *129*, 5153-5166 (and Supporting Information).
(2) Manner, V. W.; Markle, T. F.; Freudenthal, J. H.; Roth, J. P. Mayer, J. M. *Chem. Comm.* **2008**, 256-258.
(3) Warren, J. J.; Mayer, J. M. *J. Am. Chem. Soc.* **2008**, *130*, 2774-2776.
(4) http://www.glasscontour.com

temperature on a Bruker EPX CW-EPR spectrometer operating at X-band frequency, and are referenced to DPPH ($g$ = 2.0036).[5] UV/visible spectra were collected at ambient temperature using a Hewlett-Packard 8453 diode array spectrophotometer and are reported as $\lambda_{max}$ in nm (ε, $M^{-1}$ $cm^{-1}$).

**EPR Sample Preparation.** The 5,6-isopropylidne-semidehydroascorbyl radical anion (***i*Asc$^{\bullet -}$**) was generated by addition of 5.9 mg (27.3 μmol) $^{t}Bu_3PhO^{\bullet}$ to 5.1 mg (20.3 μmol) ***i*AscH$_2$** and 4.0 mg (26.2 μmol) DBU, in 1 mL $CH_3CN$. A capillary tube was charged with this solution, sealed with Apiezon H-grease and removed from the glovebox. Capillary tubes were flame-sealed immediately and stored in liquid nitrogen before data collection. EPR spectra were collected at room temperature. EPR spectra were simulated using EPR-WINSIM: NIEHS software (Figure S1);[6] the errors in the hyperfine coupling constants are estimated to be ± 0.02 G.

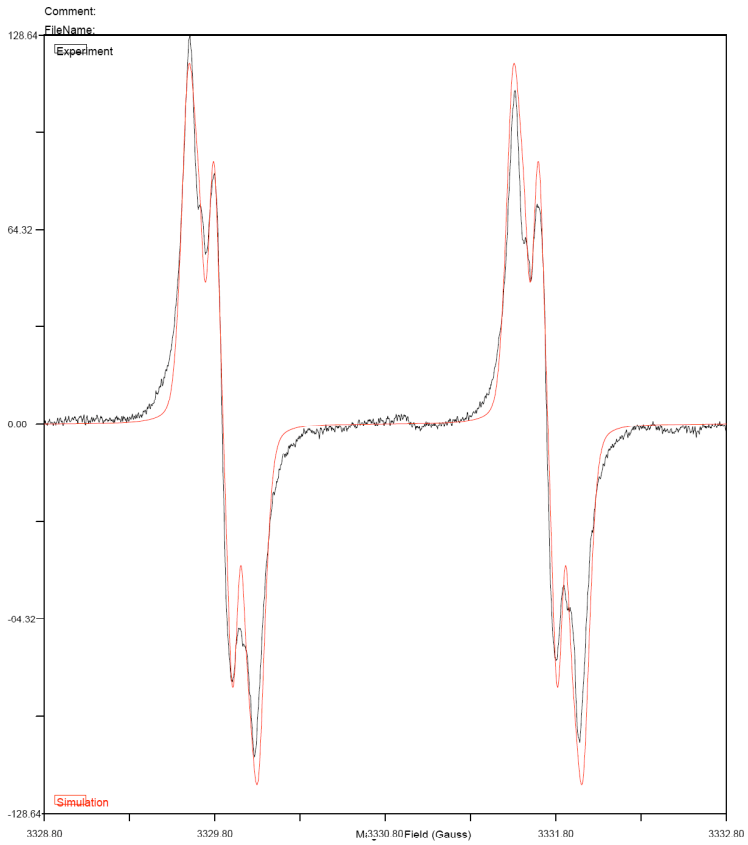


**Figure S1.** Experimental (—) and simulated (—) EPR spectra.

(5) Alger, R. S. *Electron Paramagnetic Resonance: Techniques and Applications*; Interscience: New York, NY, 1968; pp 412-413.

(6) (a) Dulig, D. R. *J. Magn. Res. B* **1994**, *104*, 105-110. (b) EPR-WinSim 2002, v. 0.98, Available: http://www.niehs.nih.gov/research/resources/software/tools/index.cfm (Accessed 04/16/08).

**Titrations for p$K_a$(*i*AscH$_2$) and p$K_a$(*i*AscH$^-$) (Figure S2).** Titrations were carried out using quartz cuvettes with Kontes Teflon$^{TM}$ stoppers. In a typical titration, 25 mL of $7.0 \times 10^{-5}$ stock solution was prepared by diluting 100 μL of 17.6 mM ***i*AscH$_2$** (or ***i*AscH$^-$**) to 25 mL in $CH_3CN$. ***i*AscH$^-$** (17.6 mM) was prepared by adding 2.7 mg of DBU to 1 mL of 17.6 mM ***i*AscH$_2$**. Six cuvettes were charged with 3 mL of the stock solution. An aliquot of concentrated base solution [10-100 equiv. for *N*-methylmorpholine (Aldrich) and 10-100 equiv. for 1,5,7-Triazabicyclo[4.4.0]dec-5-ene (TBD, Aldrich)] was placed above the Teflon$^{TM}$ stopper and the apparatus was capped with a rubber septum. Initial UV-Vis spectra were taken for each cuvette, then the reaction was initiated by opening the Teflon$^{TM}$ stopper and mixing the two solutions. Solutions were allowed to equilibrate for 30 seconds before measurement. The concentration of *N*-methylmorpholine–H$^+$ and TBD–H$^+$ were calculated by assuming mass balance. Data analysis was performed at 273 nm for p$K_a$(***i*AscH$_2$**) [$\varepsilon_{273}$(***i*AscH$_2$**) = 1400 M$^{-1}$ cm$^{-1}$, $\varepsilon_{273}$(***i*AscH$^-$**) = 11000 M$^{-1}$ cm$^{-1}$] and at 320 nm for p$K_a$(***i*AscH$^-$**) [$\varepsilon_{320}$(***i*AscH$^-$**) = 100 M$^{-1}$ cm$^{-1}$, $\varepsilon_{320}$(***i*Asc$^{2-}$**) = 2700 M$^{-1}$ cm$^{-1}$].

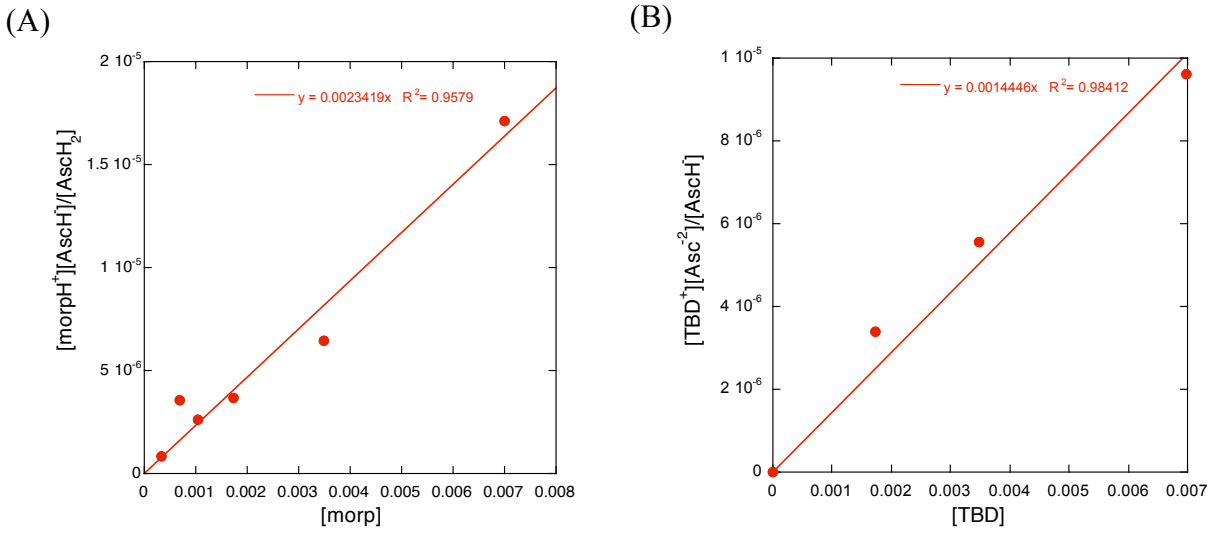


**Figure S2.** (A) p$K_a$ titration of ***i*AscH$_2$**. The slope gives $K_{eq}$ for ***i*AscH$_2$** + *N*-methylmorpholine. (B) p$K_a$ titration of ***i*AscH$^-$**. The slope gives $K_{eq}$ for ***i*AscH$^-$** + TBD.

**Electrochemistry**. Cyclic voltammograms were collected using an E2 Epsilon electrochemical analyzer (Bioanalytical Systems). Electrochemical measurements were performed in a $N_2$ filled glovebox with approximately 3 mM substrate and 0.1 M $^{n}Bu_4NPF_6$ in acetonitrile. The electrodes used were: working electrode, glassy carbon; reference electrode, 0.01M $Ag^0/AgNO_3$ in $^{n}Bu_4NPF_6/CH_3CN$ electrolyte solution; and auxiliary electrode, platinum wire. All potentials are referenced versus ferrocene (Fc) standard. The estimated errors are ± 0.020 V, unless otherwise noted. Scans were taken at 100 and 250 mV $s^{-1}$ in the absence of ferrocene. Ferrocene was added and CVs were obtained again at 250 mV $s^{-1}$, with no change in peak currents or potentials. Typical CV's for ***i*AscH**$^-$ and ***i*Asc**$^{2-}$ are shown in Figure S3.

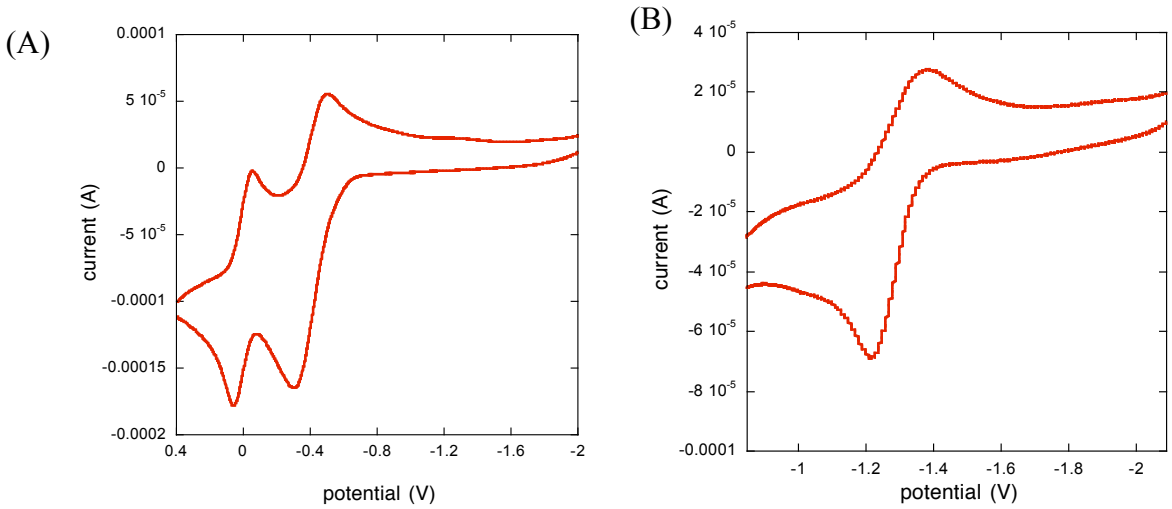


**Figure S3.** (A) Cyclic voltammogram of ***i*AscH**$^-$ in $CH_3CN$. The left-most wave at 0 V is due to $Fc^{+/0}$ internal standard (Fc = ferrocene). ***i*AscH**$^-$ was generated from addition of 1 equivalent of KO$^t$Bu to an acetonitrile solution of ***i*AscH$_2$**. (B) Cyclic voltammogram of ***i*Asc**$^{2-}$ in $CH_3CN$. ***i*Asc**$^{2-}$ was generated by addition of 2 equivalents of tetrabutylammonium hydroxide (1 M solution in methanol) to an acetonitrile solution of ***i*AscH$_2$**. Control experiments in the absence of ***i*AscH$_2$** show no signal.

**Mass Spectra (Figure S4).** Mass spectra were recorded from $CH_3CN$ solutions on a Bruker Esquire ion trap electrospray ionization mass spectrometer.

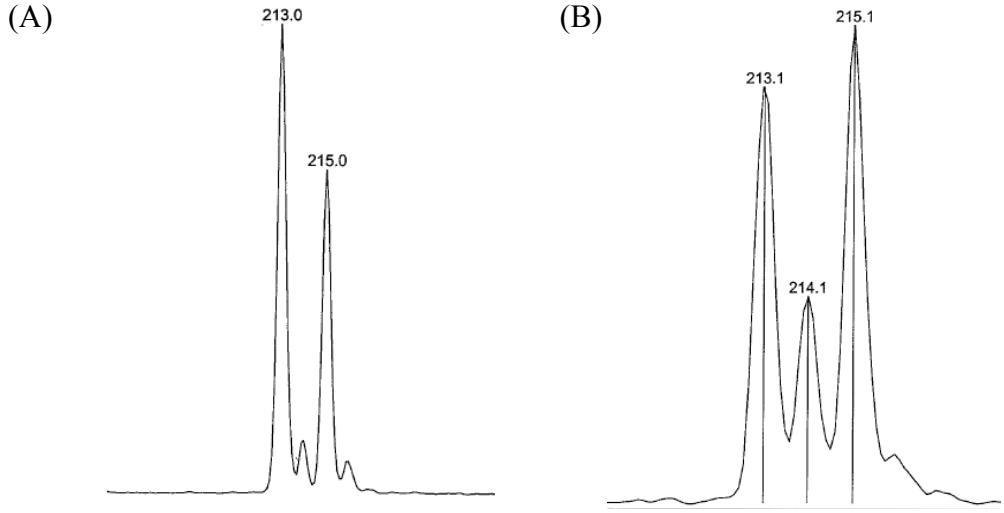


**Figure S4.** (A) Negative ion ESI mass spectrum of a mixture of 5,6-isopropylidene dehydroascorbate (***i*Asc**, m/*z* = 213) and 5,6-isopropylidene ascorbate (***i*AscH**$^-$, m/*z* = 215). (B) Negative ion ESI mass spectrum of ***i*AscH**$^-$ + $^t$Bu$_3$PhO$^\bullet$ reaction mixture *ca*. 1 hour after mixing. ***i*Asc**$^{\bullet-}$ has m/*z* = 214.

**Decomposition of *i*Asc$^{\bullet-}$ as a function of [$H_2O$] (Figure S5).** Screw-top quartz cuvettes were charged with 3 mL of acetonitrile under an inert atmosphere. ***i*AscH**$^-$ stock solution (33 μL, 13 mM) was added to give a concentration of 0.14 mM. The cuvettes were sealed with a PTFE septum, removed from the glovebox one at a time and placed in the spectrometer under flowing $N_2$. ***i*Asc**$^{\bullet-}$ was generated by addition of 50 μL of 7.6 mM $^t$Bu$_3$PhO$^\bullet$ through the septum. For runs with added water, degassed deionized water was added through the septum prior to addition of $^t$Bu$_3$PhO$^\bullet$. Water was degassed by bubbling with nitrogen for 30 minutes. Data collection was started immediately after addition of $^t$Bu$_3$PhO$^\bullet$.

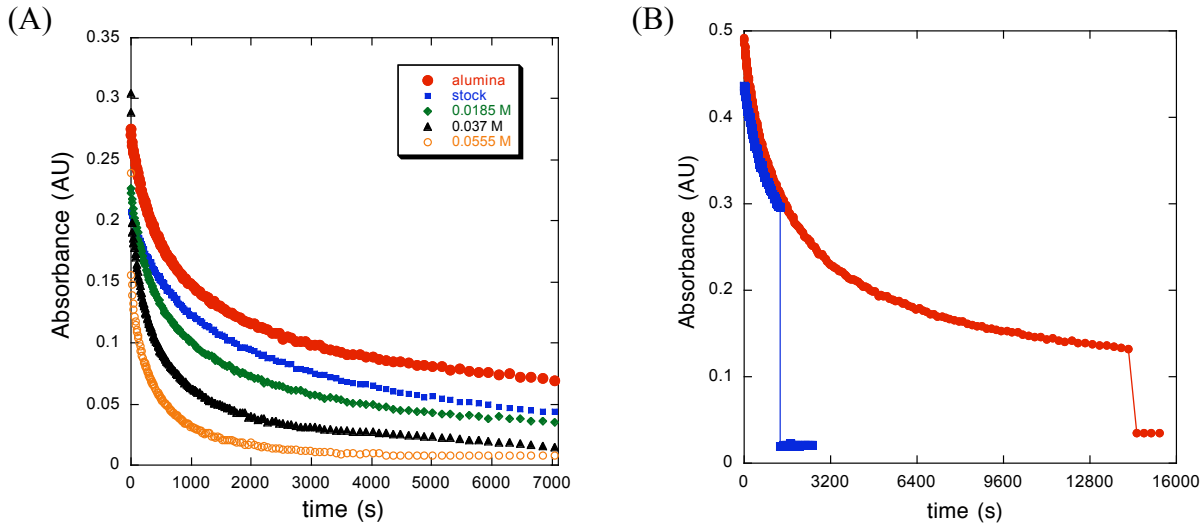


**Figure S5:** (A) Traces at 377 nm for the decay of 5,6-isopropylidene ascorbyl radical (***i*Asc**$^{\bullet-}$) as a function of water concentration. "Alumina" samples were dried by passing acetonitrile through a pipette column of activated alumina. "Stock" acetonitrile has [$H_2O$] ~ $3 \times 10^{-4}$ M (Burdick and Jackson specifications). (B) Trace at 377 nm for the decay of 0.13 mM solutions of ***i*Asc**$^{\bullet-}$, with addition of trifluoroacetic acid (TFA) after 1200 s (■) and after 14400 min (●). Final [TFA] = 0.1 mM.

**Stopped-flow kinetics, General.** Kinetic runs were performed on an OLIS RSM-1000 stopped-flow spectrophotometer. All solutions used for kinetics were prepared in a $N_2$ filled glovebox. The stopped-flow syringes were loaded in an $N_2$-filled glovebox, and removed one at a time for each respective kinetic run. Measurements were at 295 K unless otherwise indicated. For reactions at temperatures other than 295 K, all solutions were allowed to equilibrate in the water bath of the stopped-flow instrument for 5 min. The data were fit by the SPECFIT/32™ global analysis program.[7]

**Stopped-flow kinetics for *i*AscH$^-$ + TEMPO (Figure S6).** A 25 mL ***i*AscH**$^-$ (0.35 mM) in $CH_3CN$ was freshly generated from 3.7 mg and 25 μL of a 19.3 mg/mL DBU stock solution (in $CH_3CN$). $k_3$ was measured using 10-40 equivalents of TEMPO. The data were fit by the SPECFIT/32™ global analysis program[7] to a first-order kinetic model. The blue curved line in

(7) Binstead, R. A.; Zuberbühler, A. D.; Jung, B. *Specfit*, Version 3.0.38 (32-bit Windows); Spectrum Software Associates: Chapel Hill, NC, 2006.

Figure S6(B) is a plot of that global fit at a single wavelength. Pseudo-first order rate constants were plotted as a function of [TEMPO] (Figure S7) to give $k_3$ = 1720 ± 150 $M^{-1}$ $s^{-1}$.

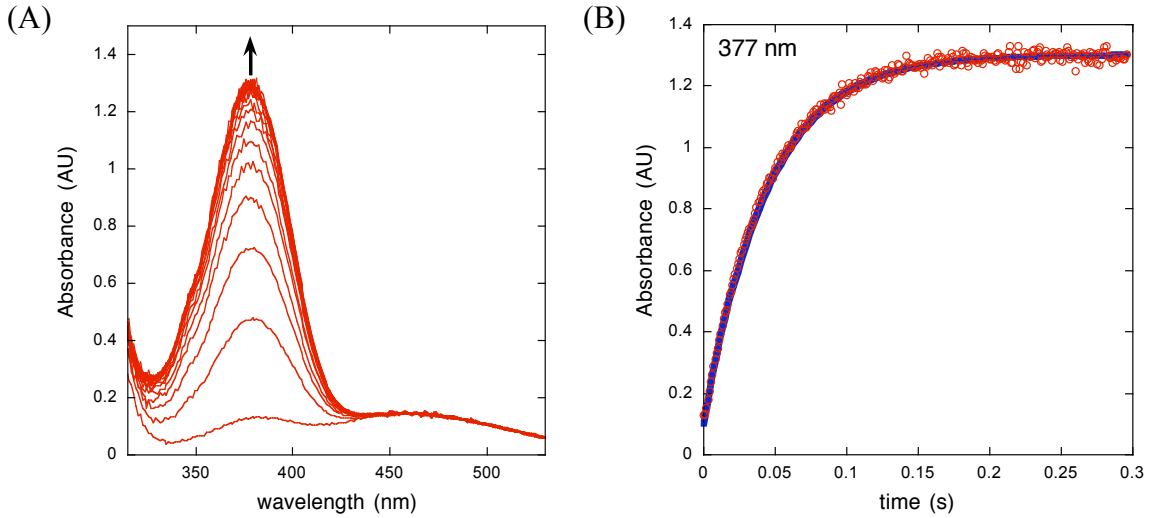


**Figure S6.** (A) Selected UV/Vis spectra for reaction between 0.35 mM ***i*AscH**$^-$ and 8.3 mM TEMPO over the course of 0.3 s. (B) Trace of the absorbance at 377 nm (O) and the fit (blue —) at that wavelength resulting from analysis with SPECFIT/32 using a first order kinetic model.

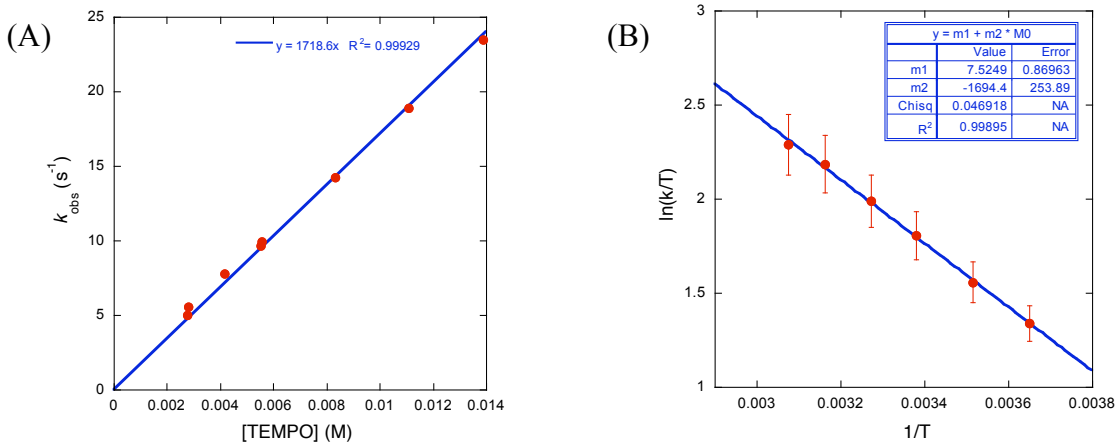


**Figure S7.** (A) Pseudo-first order plot for the reaction of 0.35 mM ***i*AscH**$^-$ and 3.5-14 mM TEMPO (10-40 equiv.) at 298 K (B) Eyring plot for the reaction of 0.35 mM ***i*AscH**$^-$ and 8.7 mM TEMPO (25 equiv.) between 274 K and 325 K.

**Measurement of the *i*AscH$^-$ + TEMPO Equilibrium Constant ($K_3$, Figure S8).** A 25 mL solution of ***i*AscH**$^-$ (0.13 mM) was generated from 1.4 mg ***i*AscH$_2$** and 25 μL of a 48 mM DBU stock solution (in $CH_3CN$). The DBU stock solution was freshly made from 7.3 mg DBU in 1 mL $CH_3CN$. $K_3$ was determined from the final absorbance of ***i*Asc$^{\bullet-}$** using stopped-flow kinetics with 1-15 equiv. of TEMPO. Stopped-flow runs at 298 K to determine $K_3$ were performed in the same manner as above. Mass balance was assumed; for instance [TEMPOH] =

[***i*Asc$^{\bullet-}$**]. The linearity of Figure S8 provides support for this assumption. Titration to determine $K_{eq}$ for *L*-Ascorbate + TEMPO were carried out analogously.

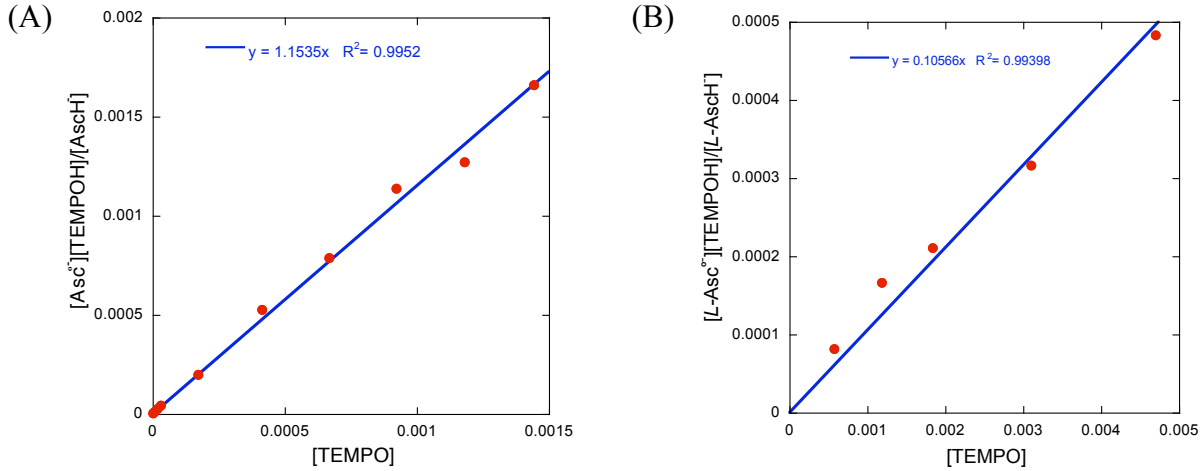


**Figure S8.** (A) Plot of [***i*Asc$^{\bullet-}$**][TEMPOH]/[***i*AscH$^-$**] vs. [TEMPO]. The slope gives the value of $K_3$ = 1.2 ± 0.2. (B) Plot of [***L*-Asc$^{\bullet-}$**][TEMPOH]/[***L*-AscH$^-$**] vs. [TEMPO]. The slope gives the value of $K_{eq}$ = 0.11 ± 0.07.

**Stopped-flow kinetics for *i*AscH$^-$ + $^t$Bu$_3$PhO$^\bullet$ or 2,6-$^t$Bu$_2$-4-MeOC$_6$H$_2$O$^\bullet$ (Figures S9 and S10).** A 25 mM stock solution of ***i*AscH$^-$** (in $CH_3CN$) was freshly generated from 5.4 mg ***i*AscH$_2$** and 3.8 mg DBU in 1 mL $CH_3CN$. A 25 mM stock solution of $^t$Bu$_3$PhO$^\bullet$ was prepared by dissolving 5.6 mg of solid $^t$Bu$_3$PhO$^\bullet$ in 1 mL of $CH_3CN$. A 62 μM solution of ***i*AscH$^-$** for stopped-flow spectrophotometry was prepared by dilution of 50 μL ***i*AscH$^-$** stock solution with 10 mL $CH_3CN$. Similarly, a 38 μM solution of $^t$Bu$_3$PhO$^\bullet$ was prepared by dilution of 35 μL stock solution with 10 mL $CH_3CN$.

$k_1$ was measured using less than 1 equivalent of $^t$Bu$_3$PhO$^\bullet$ because excess phenoxyl appears to react rapidly with ***i*Asc$^{\bullet-}$**. The reaction of 62 μM ***i*AscH$^-$** and 38 μM $^t$Bu$_3$PhO$^\bullet$ was (50 ± 5)% complete in the dead time of our stopped-flow spectrometer (~3 ms). This was determined from the first spectrum using the extinction coefficients of ***i*Asc$^{\bullet-}$** (from reaction with TEMPO) and $^t$Bu$_3$PhO$^\bullet$.[2] To analyze the kinetic data, the starting spectrum was set as time = 0, with starting concentrations of 43 μM ***i*AscH$^-$** and 19 μM $^t$Bu$_3$PhO$^\bullet$. The data and kinetic fit are shown in Figure S9. Figures S9(B) also indicates the absorbance expected prior to any reaction, by the horizontal (black) bar around time = 0. The data were fit by the SPECFIT/32™ global analysis program to a simple second-order kinetic model (blue curved line in Figure S9(B)). The quality of the fit was high, based on the good agreement of the SPECFIT-calculated component spectra for ***i*Asc$^{\bullet-}$** and $^t$Bu$_3$PhO$^\bullet$ with the known spectra. Reactions at different concentrations of ***i*AscH$^-$** (62 μM and 0.28mM) and $^t$Bu$_3$PhO$^\bullet$ (44 μM and 0.19 mM, respectively) gave the same second-order rate constants within error: $k_1 = (3.4 \pm 0.5) \times 10^6$ M$^{-1}$ s$^{-1}$.

The kinetics of 0.28 mM ***i*AscH$^-$** plus 0.16 mM 2,6-$^t$Bu$_2$-4-MeOC$_6$H$_2$O$^\bullet$ [from 10 μL of 0.2 M 2,6-$^t$Bu$_2$-4-MeOC$_6$H$_2$O$^\bullet$ (in benzene) in 10 mL $CH_3CN$] was performed and analyzed similarly (Figure S10). This reaction was found to be (20 ± 5)% complete at the time of the first spectrum. Reactions at different concentrations of ***i*AscH$^-$** (62 μM and 0.28mM) and 2,6-$^t$Bu$_2$-4-

$MeOC_6H_2O^{\bullet}$ (40 μM and 0.19 mM, respectively) gave the same second-order rate constants within error: $k = (5.3 \pm 0.5) \times 10^5\ M^{-1}\ s^{-1}$.

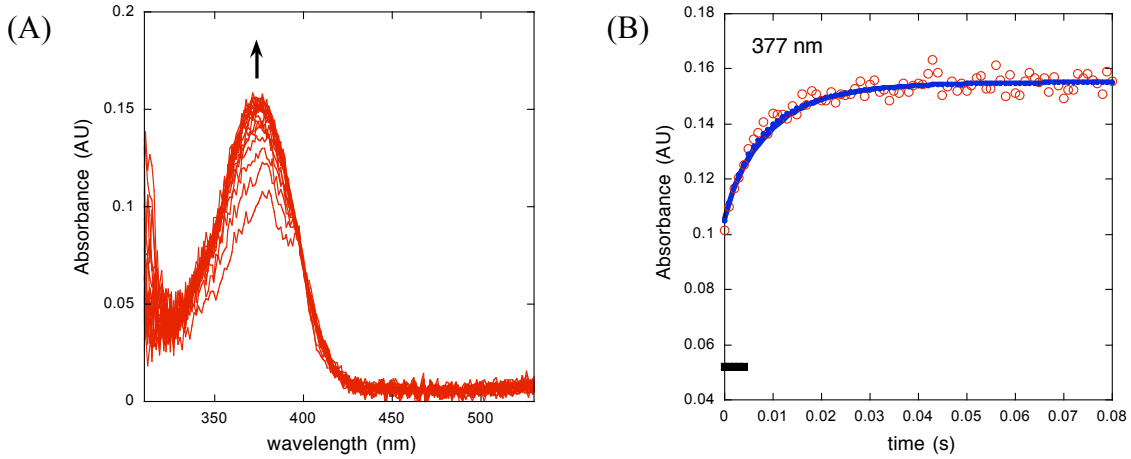


**Figure S9.** (A) UV/Vis spectra for reaction between 62 μM ***i*AscH**$^-$ and 38 μM $^tBu_3PhO^{\bullet}$ over the course of 0.08 s. The reaction was (50 ± 5)% complete within the mixing time of the stopped-flow. (B) Trace at 377 nm of the data (○) and fit resulting from analysis with SPECFIT/32 using the second-order kinetic model described above (blue —). The absorbance expected prior to any reaction is indicated by the horizontal (black) bar around time = 0, which was set to be the time of the first spectrum after complete mixing.

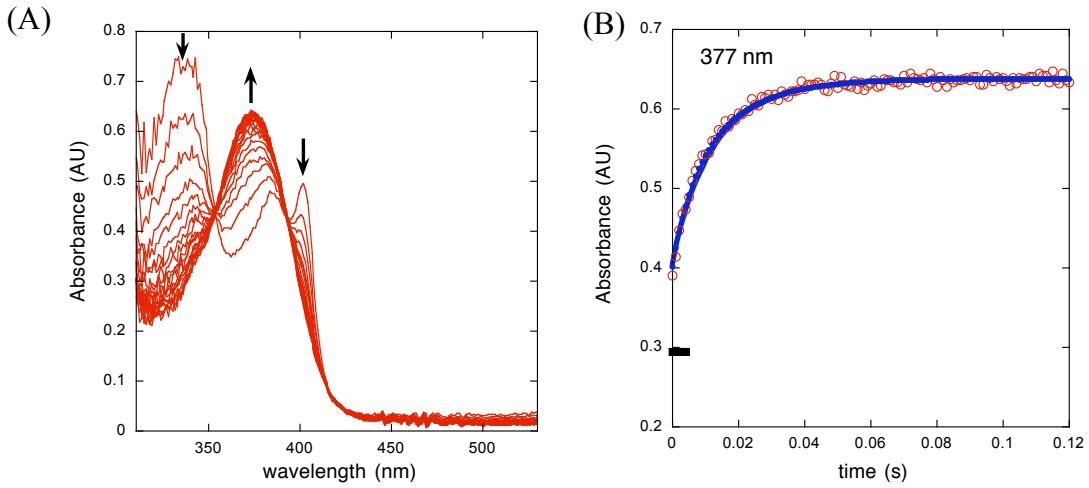


**Figure S10.** (A) UV/Vis spectra for reaction between 0.28 mM ***i*AscH**$^-$ and 0.17 mM 2,6-$^tBu_2$-4-$MeOC_6H_2O^{\bullet}$ over the course of 0.12 s. The reaction was (20 ± 5)% complete within the mixing time of the stopped-flow. (B) Trace at 377 nm of the data (○) and fit resulting from analysis with SPECFIT/32 using the second-order kinetic model described above (blue —). The absorbance expected prior to any reaction is indicated by the horizontal (black) bar around time = 0, which was set to be the time of the first spectrum after complete mixing.

**Kinetic Isotope Effect (KIE) Measurements (Figure S11).** Measurement of rates for deuterium transfer from ***i*AscD**$^-$ were performed as described above, using ***i*AscD$_2$** in $CH_3CN$ containing 0.1% $CD_3OD$ (to ensure high isotopic enrichment). Control experiments showed that the kinetics of the protio substrate are unaffected by the presence of 0.1% $CH_3OH$. ***i*AscD$_2$** was

prepared by stirring ***i*AscH$_2$** with $CH_3OD$ under an inert atmosphere. Residual methanol was removed under vacuum and fresh $CH_3OD$ was vacuum transferred onto the ***i*AscH$_2$/D$_2$** three times. After the third addition the solvent was removed and the product was dried under vacuum. The deuterium enrichment was found to be (95 ± 10)% by $^1$H NMR in dry $CD_3CN$.

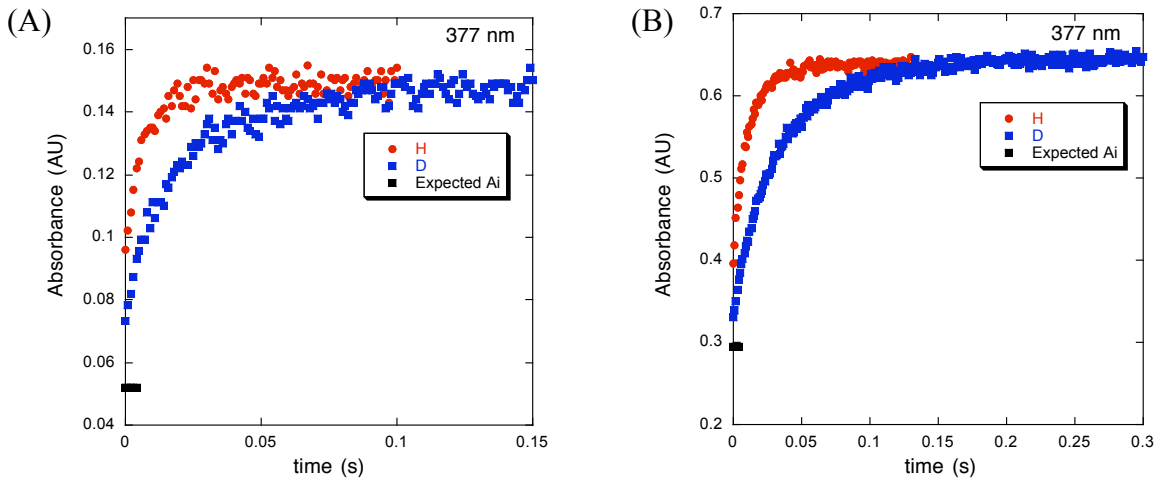


**Figure S11.** Kinetic traces at 377 nm for the reactions between 38 μM $^t$Bu$_3$PhO$^\bullet$ and either 62 μM ***i*AscH$^-$** (red circles, ●) or 62 μM ***i*AscD$^-$** (blue squares, ■). Significant reaction occurs within the mixing time of the instrument. From static UV/Vis measurements, both protio and deutero samples have the same starting absorbance, as indicated by the black line near time = 0, which was set to be the time of the first spectrum after complete mixing. (B) Comparison of kinetic traces at 377 nm for the reactions between 0.16 mM 2,6-$^t$Bu$_2$-4-MeOC$_6$H$_2$O$^\bullet$ and either 0.22 mM ***i*AscH$^-$** (red circles, ●) or 0.22 mM ***i*AscD$^-$** (blue squares, ■).

**p$K_a$ and $E°$ values for TEMPOH in $CH_3CN$**. $E°(TEMPOH^{\bullet+/0})$ in acetonitrile vs. $AgNO_3/Ag^0$ was reported by Semmelhack and co-workers to be 0.8 V (0.71 V *vs*. $Fc^{+/0}$).[8] $E°(TEMPO^{\bullet/-})$ = -1.91 V in acetonitrile vs. $Fc^{+/0}$ was reported by Mori and co-workers.[9] The p$K_a$ of TEMPOH in DMSO was reported by Bordwell and co-workers;[10] the p$K_a$ in acetonitrile was estimated from this value following the method of Chantooni and co-workers [p$K_a$($CH_3CN$) = p$K_a$(DMSO) + 10.2].[11] Using the above data and a closed thermochemical cycle [1.37[p$K_a$(TEMPOH)–p$K_a$(TEMPO)] – 23.1[$E°(TEMPOH^{\bullet+/0})$– $E°(TEMPO^{\bullet/-})$= 0 ] give p$K_a$(TEMPO) = -3 in $CH_3CN$.

**Thermochemistry and Stepwise *vs.* Concerted Mechanism for $^t$Bu$_3$C$_6$H$_2$O$^\bullet$ + *i*AscH$^-$.** Niyazymbetov et. al have reported the redox potential for $^t Bu_3C_6H_2O^{-/\bullet}$ = -0.71 V *vs*. $Fc^{+/0}$ in $CH_3CN$.[12] Osako and co-workers reported the redox potential for the corresponding phenol $^t Bu_3C_6H_2OH^{\bullet+/0}$ = 1.58 V *vs*. SCE in $CH_3CN$ (0.94 V *vs*. $Fc^{+/0}$).[13] The p$K_a$ of $^t Bu_3C_6H_2OH$ in DMSO was reported by Bordwell,[14] and converted to a p$K_a$ in acetonitrile using the method of Chantooni.[11] Applying these data to a closed thermochemical cycle (as above) give p$K_a$($^t Bu_3C_6H_2O^{\bullet+}$) = 0.3 in acetonitrile solvent.

The above thermochemical data can be used to indicate a likely reaction mechanism for the net hydrogen atom transfer (HAT) mechanism for the reduction of $^t Bu_3C_6H_2O^\bullet$ by ***i*AscH**$^-$. In principle, the reduction of $^t Bu_3C_6H_2O^\bullet$ by ***i*AscH**$^-$ could occur by three mechanisms: by initial proton transfer followed by electron transfer (PT-ET), by initial ET followed by PT or by a CPET process. The ground state free energy changes ($\Delta G^\circ$) for initial PT or initial ET can be used to estimate *minimum* activation barriers, since $\Delta G^\ddagger \geq \Delta G^\circ$. Initial PT to give ***i*Asc**$^{2-}$ and $^t Bu_3PhOH^{\bullet+}$ is uphill by 34 kcal mol$^{-1}$. Likewise, initial ET to give ***i*AscH**$^\bullet$ and $^t Bu_3PhO^-$ is uphill by 11 kcal mol$^{-1}$. The difference between the minimum (11 kcal mol$^{-1}$) and observed ($\Delta G_1^\ddagger$ = 8.5 kcal mole$^{-1}$) activation barriers is small, however it is unlikely that initial ET would have $\Delta G^\ddagger_{ET} = \Delta G^\circ_{ET}$. A primary kinetic isotope effect, $k_H/k_D$ 3.2 ± 0.6 also argues against initial (rate limiting) electron transfer.

(8) Semmelhack, M. F.; Chou, C. S.; Cortes, D. A. *J. Am. Chem. Soc.* **1983**, *105*, 4492-4494.
(9) Mori, Y.; Sakaguchi, Y.; Hayashi, H. *J. Phys. Chem. A* **2000**, *104*, 4896-4905.
(10) Bordwell, F. G.; Liu, W.-Z. *J. Am. Chem. Soc.* **1996**, *118*, 10819-10823.
(11) Chantooni, M. K., Jr.; Kolthoff , I. M. *J. Phys. Chem.* **1976**, *80*, 1306-1310.
(12) Niyazymbetov, M. E.; Evans, D. H. *J. Chem. Soc. Perkin Trans.* **1993**, *2*, 1333-1338.
(13) Osako, T.; Ohkubo, K.; Taki, M.; Tachi, Y.; Fukuzumi, S.; Itoh, S. *J. Am. Chem. Soc.* **2003**, *125*, 11027-11033.
(14) Bordwell, F. G.; Cheng, J.-P. *J. Am. Chem. Soc.* **1991**, *113*, 1736-1743.

**Aqueous Thermochemistry of *L*-Ascorbate (Scheme S1).** The first and second p$K_a$'s of *L*-ascorbic acid are reported by Khan and Martell as p$K_a$(***L*-AscH$_2$**) = 4.0 and p$K_a$(***L*-AscH$^-$**) = 11.4 at 0.1 M ionic strength and 298 K.[15] p$K_a$(***L*-AscH$^\bullet$**) = -0.45 was reported by Laroff *et al.*[16]

Steenken and Neta have reported $E$(***L*-Asc$^{\bullet-}$/*L*-Asc$^{2-}$**) = 0.015 V at pH 13.5. Since p$K_a$(***L*-AscH$^-$**) = 11.4, $E_{pH13.5}$(***L*-Asc$^{\bullet-}$/*L*-Asc$^{2-}$**) ≈ $E°$(***L*-Asc$^{\bullet-}$/*L*-Asc$^{2-}$**). Wardman has independently calculated $E°$(***L*-Asc$^{\bullet-}$/*L*-Asc$^{2-}$**) = 0.019 V from Clark's[17] estimate of $E_m$ = 0.40 ± 0.01 V (midpoint potential at pH 0), the two p$K_a$ values and an estimate of $K_{eq}$ for disproportionation of ***L*-Asc$^{\bullet-}$**.[18]

$E°$(***L*-AscH$^\bullet$/*L*-AscH$^-$**) = 0.720 is calculated from these $E°$ and p$K_a$ values, using the edges of Scheme S1 as a thermochemical cycle: 1.37[p$K_a$(***L*-AscH$^-$**)–p$K_a$(***L*-AscH$^\bullet$**)] – 23.1[$E°$(***L*-AscH$^\bullet$/*L*-AscH$^-$**)–$E°$(***L*-Asc$^{\bullet-}$/*L*-Asc$^{2-}$**) = 0.

Williams,[19] Creutz,[20] and Njus[21] have independently derived similar thermochemical values, which yield the same homolytic bond strengths as shown below. Errors in homolytic bond strengths are estimated to be approximately ± 1.5 kcal mol$^{-1}$.

**Scheme S1: Thermochemistry of *L*-Ascorbic Acid in H$_2$O.**

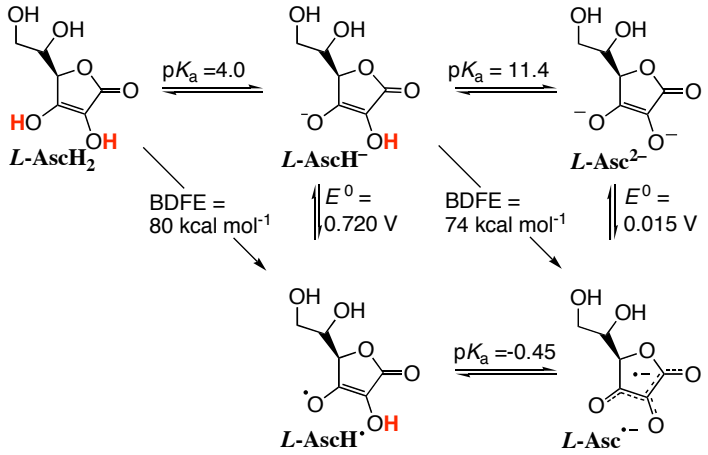


(15) Khan, M. M. T.; Martell, A. E. *J. Am. Chem. Soc.* **1967**, *89*, 4176-4185
(16) Laroff, G. P.; Fessenden, R. W.; Schuler, R. H. *J. Am. Chem. Soc.* **1972**, *94*, 9062-9073.
(17) Clark, W. M. *Oxidation-Reduction Potentials of Organic Systems;* Williams and Wilkins: Baltimore, MD, 1960; pp 470.
(18) Wardman, P. *J. Phys. Chem. Ref. Data.* **1989**, *18*, 1637-1755.
(19) Williams, N. H.; Yandell, J. K. *Aust. J. Chem.* **1982**, *35*, 1133-1144.
(20) Creutz, C. *Inorg. Chem*. **1981**, *20*, 4449-4452.
(21) Njus, D.; Kelley, P. M. *FEBS Letters*, **1991**, *284*, 147-151.